Cluster Thomas-Ehrman effect in mirror nuclei

M. Nakao,[1] H. Umehara,[1,2] S. Ebata,[3] and M. Ito[1,4,*]

[1]*Department of Pure and Applied Physics, Kansai University, Yamatecho, 3-3-35, Suita 564-8680, Japan*

[2]*Department of Physics, Osaka University, Machikaneyama-cho, 1-1, Toyonaka 560-0043, Japan*

[3]*Laboratory for Advanced Nuclear Energy, Institute of Innovative Research, Tokyo Institute of Technology, 2-12-1-N1-16 Ookayama, Meguro-ku 152-8550, Japan*

[4]*Research Center for Nuclear Physics (RCNP), Osaka University, Mihogaoka 10-1, Suita 567-0047, Japan*

(Received 14 January 2018; revised manuscript received 16 August 2018; published 26 November 2018)

The Coulomb shift is analyzed for the mirror cluster systems of $^{18}\mathrm{O} = \alpha + {}^{14}\mathrm{C}$ and $^{18}\mathrm{Ne} = \alpha + {}^{14}\mathrm{O}$ by applying the orthogonality condition model (OCM). The OCM calculation clearly predicts the suppressed excitation energy of the higher 0^+ states in the proton-rich system of ^{18}Ne. This results can be interpreted in terms of the extension of the Thomas-Ehrman shift (TES), which is discussed in $^{17}\mathrm{O} = {}^{16}\mathrm{O} + N$ and $^{17}\mathrm{F} = {}^{16}\mathrm{O} + P$, to the cluster degrees of freedom. A combination of the cluster TES and the monopole transition is proposed as an experimental probe to identify the cluster structure in mirror systems.

DOI: 10.1103/PhysRevC.98.054318

I. INTRODUCTION

In a ground state of nuclei, a mean-field picture is realized in which nucleons, such as neutrons (N) and protons (P), perform independent particle motions in a self-consistent mean field. In the mean-field picture, neutrons in S-wave orbit often induce anomalous phenomena. A typical example of S-wave anomaly is the halo or skin phenomenon, which is generated by the spatially extended wave function in the S orbit [1]. An interesting phenomenon, which arises from the extended S orbit, can also be seen in the Coulomb shift for the mirror systems. The famous example is "Thomas-Ehrman shift (TES)," which was discussed in the mirror pair of $^{17}\mathrm{O} = {}^{16}\mathrm{O} + N$ and $^{17}\mathrm{F} = {}^{16}\mathrm{O} + P$ [2]. Since the wave function in the S orbit is spatially extended, the effect of the Coulomb interaction is suppressed in a proton-rich system. As a result of this suppression, the excitation energy of the $1/2^+$ ($1s_{1/2}$) state in the proton-rich ^{17}F seems to be compressed in comparison to the neutron-rich ^{17}O [2].

On the contrary, the α-cluster structures are well known to appear in the excited states of light-mass systems. The α particle is a building block in constructing the intrinsic structures of nuclei because of its stable and inert property. The α-cluster structures have been extensively discussed in the $4N$ systems, which have the multiple mass number of the α particle [3–5], such as $^{8}\mathrm{Be} = 2\alpha$, $^{12}\mathrm{C} = 3\alpha$, $^{16}\mathrm{O} = \alpha + {}^{12}\mathrm{C}$, and $^{20}\mathrm{Ne} = \alpha + {}^{16}\mathrm{O}$. These α-cluster structures mainly appear in the excited 0^+ states below 15 MeV in the excitation energy.

α-cluster structures appear according to Ikeda's threshold rule [6]; specifically, a possible cluster configuration emerges at the excitation energy near the corresponding threshold for cluster decay. In the α-cluster structure, the α particle and the residual nuclei are weakly coupled. This weak-coupling feature leads to a large extension of the wave function of the cluster relative motion with a large mixture of the S-wave component. In this situation, the Coulomb interaction is not so effective, and the suppressed Coulomb shift, which is similar to the phenomenon discussed in ^{17}O-^{17}F, is expected to be observed. Therefore, it is interesting to extend the viewpoint of the TES, which is discussed in the single-particle picture, to the α-clustering phenomena. If the TES occurs in the α-cluster states, we will observe the compressed excitation energy of the excited 0^+ states in the proton-rich system. In fact, such a compression of the excitation energy for the excited 0^+ states has been briefly discussed in ^{10}Be-^{10}C from the viewpoint of the covalent molecular picture [7].

In the present paper, we extend the analysis of the Coulomb shift studied in ^{10}Be-^{10}C to the heavier systems, such as ^{18}O-^{18}Ne, which are handled by the cluster models of $\alpha + {}^{14}\mathrm{C}$ and $\alpha + {}^{14}\mathrm{O}$, respectively. In ^{18}O, the $\alpha + {}^{14}\mathrm{C}$ structure has already been discussed by the full microscopic model in which the antisymmetrization among all the nucleons is completely taken into account [8–10]. However, the energy levels of the excited 0^+ states, which have the well-developed $\alpha + {}^{14}\mathrm{C}$ structure, are much higher than the observed 0^+ levels, and hence, the direct comparison of the theory with the experiment is still difficult. In addition, the recent shell model [11] or three-body model [12] for $^{18}\mathrm{O} = {}^{16}\mathrm{O} + N + N$ also had difficulty reproducing three bound 0^+ levels.

In view of the previous results of the full microscopic calculations, we consider that it is important to introduce the semimicroscopic model. The orthogonality condition model (OCM), which is a kind of semimicroscopic models, is a very useful and powerful model [13]. The OCM application to ^{18}O was performed by Furutani *et al.*, but the scattering boundary condition for the unbound continuum was not considered [14]. Here we employ the OCM plus absorbing boundary condition (ABC), which is a powerful tool to handle the unbound continuum, and apply the OCM + ABC to the analysis of the mirror cluster systems of ^{18}O-^{18}Ne. Preliminarily, the

*itomk@kansai-u.ac.jp

OCM + ABC analysis of ^{18}O-^{18}Ne has been performed [15], and we formulate the OCM calculation in the more complete form. In this article, we mainly analyze the 0^+ energy levels, although there are many finite spin-parity states, which are considered to have the $\alpha + {}^{14}$C cluster structure. The analysis focusing on the 0^+ states is because the most prominent mixture of the S-wave component arises in the $\alpha + {}^{14}\mathrm{C}_{\mathrm{g.s.}}$ relative motion with the spin parity of 0^+ and hence we can expect the maximal effect of the suppressed Coulomb shift due to the dilute α-cluster formation.

II. THEORETICAL FRAMEWORK

A. OCM formulation

We apply the OCM to the $\alpha + {}^{14}$C and $\alpha + {}^{14}$O systems. In the strict treatment of the OCM, the so-called Pauli-allowed states are constructed by solving the eigenvalue problem of the norm kernels [13]. In the present analysis, we construct the Pauli-allowed states in a simple manner based on Elliott's SU(3) algebra [16]. As for the internal configurations of the binary clusters, we assume the lowest shell-model configurations, such as $(0s)^4\pi(0p)^4\nu(0p)^6$ [$(0s)^4\pi(0p)^6\nu(0p)^4$] and $(0s)^4$ for the ^{14}C (^{14}O) nucleus and the α particle, respectively. The internal configuration of ^{14}C (^{14}O) is set to $(\lambda, \mu) = (0, 2)$ in the SU(3) irreducible representation of the harmonic-oscillator (HO) wave function [16]. In this representation, ^{14}C (^{14}O) is possible to take the intrinsic angular momenta of $I^\pi = 0^+$ and 2^+, which correspond to the ground and first excited states, respectively.

In the following, we explain the OCM formulation for the $\alpha + {}^{14}$C system because the extension to the $\alpha + {}^{14}$O system can be achieved in a straightforward manner. The Pauli-allowed states of the total system, which are composed of α and ^{14}C, must have the total HO quanta of $N \geqslant 6$ in the $\alpha - {}^{14}$C relative motion. The $N = 6$ state corresponds to the partially allowed state, whereas the quantum states with $N \geqslant 8$ are the completely allowed states for the positive parity. The SU(3) representation for the partially allowed states can be generated according to the following coupling scheme of the SU(3) irreducible representation:

$$(0, 2) \otimes (6, 0) = (4, 0), \tag{1}$$

where (0,2) corresponds to the irreducible representation for the internal state whereas (6,0) denotes the representation for the relative motion of the oscillator quanta $N = 6$. The totally coupled state of (4,0) corresponds to the lowest shell-model state of $^{18}\mathrm{O} = {}^{16}\mathrm{O} \otimes \nu(1s0d)^2$.

By combining Eq. (1) and the angular momentum coupling of $\mathbf{I}$ and $\mathbf{L}$, which represent the internal spin of ^{14}C and the orbital spin of $\alpha - {}^{14}$C, respectively, we can expand the $N = 6$ partially allowed state [$\Phi_{\mathrm{PA}}(N = 6)$] in terms of the channel wave function. In the case of zero total spin ($\mathbf{I} + \mathbf{L} = \mathbf{J} = 0$), which is the main subject in the present analysis, the expansion becomes

$$\Phi_{\mathrm{PA}}^{J=0}(N = 6) = \frac{1}{2}\phi_{0,0}R_0(N = 6) + \frac{\sqrt{3}}{2}\phi_{2,2}R_2(N = 6). \tag{2}$$

Here $\phi_{I,L}$ denotes the channel wave function with the internal spin (I) and the relative spin (L) for $\alpha + {}^{14}$C, whereas R_L means the radial HO wave function with $N = 6$. Thus, the partially allowed state contains the dominant component of the $^{14}\mathrm{C}(I^\pi = 2^+)$ channel ($\sim$75%). Equation (2) represents an example of the duality of the compact shell-model configuration (left-hand side) and the cluster configurations (right-hand side) in which two structures coexist in the ground state of nuclear systems. In a naive mean-field picture, the ^{18}O nucleus is a system of an ^{16}O core plus valence-two nucleons, but this nucleus potentially contains the cluster excitation degrees of freedom.

B. Nuclear interaction

After constructing the partially allowed state, the total wave function is expanded by the completely allowed states and the partially allowed state, and the coupled-channel (CC) equations are solved. In the CC calculations, the nuclear potential of α and ^{14}C is calculated from the double-folding (DF) model [17], which is symbolically written as a function of the $\alpha - {}^{14}$C relative coordinate $\mathbf{R}$,

$$U_{\mathrm{DF}}(\mathbf{R}) = \iint \rho_\alpha(\mathbf{r}_\alpha)\rho_{14}(\mathbf{r}_{14}) \cdot v_{\mathrm{NN}}^{\mathrm{DDM3Y}}(s, \rho)d\mathbf{r}_\alpha d\mathbf{r}_{14}, \tag{3}$$

with the relative coordinate of interacting pair nucleons (s), which is defined by $s = |\mathbf{r}_{14} - \mathbf{r}_\alpha - \mathbf{R}|$. Here $\mathbf{r}_\alpha$ ($\mathbf{r}_{14}$) denotes a coordinate measured from the center of mass in α (^{14}C). $\rho_\alpha(\mathbf{r}_\alpha)$ is the density of the α particle, which reproduces the charge form factor of the electron scattering, whereas $\rho_{14}(\mathbf{r}_{14})$ represents the density of ^{14}C calculated from the HO-type distribution. The HO density of ^{14}C is designed to reproduce the observed matter radius $r_{\mathrm{rms}} = 2.30$ fm, which is obtained from the analysis of the interaction cross section [18]. In Eq. (3), $v_{\mathrm{NN}}^{\mathrm{DDM3Y}}$ represents the effective nucleon-nucleon (NN) interaction of the DDM3Y (density-dependent Michigan three-range Yukawa) interaction [19–21]. Here we employ the target density approximation in which the α-particle density is neglected [22]. The DF potential with a normalization factor of $N_R \sim 0.8$ nicely reproduces the angular distribution of the elastic scattering [15].

The DF potential in Eq. (3) with the normalization factor of $N_R \sim 0.8$ is used for the ground channel of $\alpha + {}^{14}\mathrm{C}(0^+)$, but we assume the same density distribution (and DF potential) in the excited channel of $\alpha + {}^{14}\mathrm{C}(2^+)$ for simplicity. The coupling potential of $^{14}\mathrm{C}(0^+) \rightarrow {}^{14}\mathrm{C}(2^+)$ is constructed by the differential function of Eq. (3) with the strength of -0.2 fm. Above the α-decay threshold, the ABC [23–25] is applied to identify the resonance parameters, such as the resonance energy E_{R} and the decay width Γ_{R}.

III. RESULTS

The calculated energy spectra for the $J^\pi = 0^+$ state is shown in Fig. 1. The OCM calculation reproduces the binding energy of the ground 0_1^+ state (-6.2 MeV) with respect to the α-decay threshold (dashed line). The root-mean-squared radius of the theoretical 0_1^+ state is $r_{\mathrm{rms}} = 2.56$ fm, which is

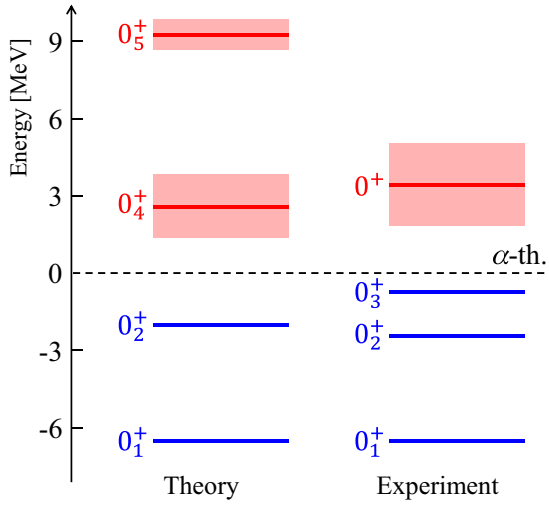

FIG. 1. Energy spectra in $^{18}\mathrm{O} = \alpha + {}^{14}\mathrm{C}$. The left and right levels are the results of the theoretical calculation and the experimental observations, respectively. The dashed line shows the α threshold, whereas the shades attached to the resonant levels represent the decay width.

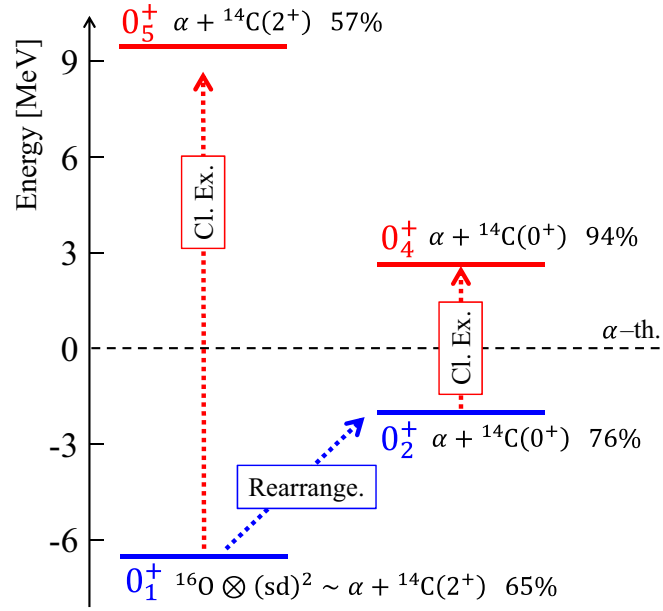

FIG. 2. Excitation scheme of 0^+ levels in $\alpha + {}^{14}\mathrm{C}$. The horizontal dashed line shows the α threshold. The number attached to the individual levels means the population of the dominant channel component. The dotted arrows with the boxes represent the excitation schemes, such as the cluster relative excitation (Cl. Ex.) and the rearrangement (Rearrange.). See the text for details.

obtained from the empirical value of $r_{\mathrm{rms}} = 1.36\,\mathrm{fm}$ for the α particle and the radius of the employed $^{14}\mathrm{C}$ density $r_{\mathrm{rms}} = 2.30\,\mathrm{fm}$. The calculated radius nicely reproduces the observed radius, such as $r_{\mathrm{rms}} = 2.59\,\mathrm{fm}$ [26]. The first excited 0_2^+ state appears at the binding energy of $E = -1.95\,\mathrm{MeV}$, which corresponds to the observed 0_2^+ level ($-2.60\,\mathrm{MeV}$). The 0_2^+ state is difficult to reproduce in the previous shell-model calculation [11] and the extended three-body calculation [12], which employ the $^{16}\mathrm{O}$ core plus two neutrons. The bound 0_1^+ and 0_2^+ states are reproduced, but the 0_3^+ state is missing in the present calculation. The reason why 0_3^+ is missing is discussed later.

On the contrary, in the unbound region, two resonant 0^+ states are obtained in the present calculation: the resonances at $E_{\mathrm{R}} \sim 2.5\,\mathrm{MeV}$ and at $E_{\mathrm{R}} = 9.3\,\mathrm{MeV}$. We label the former and latter resonances the 0_4^+ and 0_5^+ states, respectively, because of missing 0_3^+ in our calculation. The 0_4^+ level, which was not obtained in the previous calculation [14], exists around the Coulomb barrier of the $\alpha + {}^{14}\mathrm{C}_{\mathrm{g.s.}}$ ($L = 0$) channel with a broad decay width of $\Gamma_{\mathrm{R}} \sim 2.5\,\mathrm{MeV}$. Since the width of the 0_4^+ state is broad, the precise evaluation of the resonance parameters is a little difficult in the ABC method. Although the values of E_{R} and Γ_{R} calculated for 0_4^+ are rough estimates, a broad 0^+ resonance is observed in the same energy region of the $\alpha + {}^{14}\mathrm{C}$ elastic scattering, which is plotted by 0^+ with a shade above the α threshold (Experiment) [27]; the observed energy and width are $E_{\mathrm{R}} = 3.7\,\mathrm{MeV}$ ($E_{\mathrm{ex}} = 9.9\,\mathrm{MeV}$) and $\Gamma_{\mathrm{R}} = 3.2\,\mathrm{MeV}$, respectively. The energy and the width in theory seem to be consistent with those in the experimental observation, although the energies in theory are little underestimated in comparison to the experimental energy.

Concerning the 0^+ resonance, there is another observation of the 0^+ state around the same energy region ($E_{\mathrm{R}} = 1.57\,\mathrm{MeV}$) in the multinucleon transfer reaction [28], but its decay width is about 10 keV, which is much sharper than the calculated width. We have artificially varied the computational parameters, but it is difficult to reproduce the resonance with a width of 10 keV. Thus, we consider that the sharp 0^+ resonance in the multinucleon transfer does not correspond to the calculated 0_4^+ state, which is obtained by the present $\alpha + {}^{14}\mathrm{C}$ model.

The picture of the excitation scheme is summarized in Fig. 2. Basically, the ground 0_1^+ state has a compact structure of the shell-model state with $^{16}\mathrm{O} \otimes \nu(1s0d)^2$, but it is equivalent to the partially allowed state of $N = 6$ in the cluster basis according to Eq. (2). The main component of the ground 0_1^+ state is not the $\alpha + {}^{14}\mathrm{C}_{\mathrm{g.s.}}$ channel but the $\alpha + {}^{14}\mathrm{C}(2^+)$ channel (65%) because of Pauli's exclusion principle.

The rearrangement of the mixing components occurs in the 0_2^+ state; specifically, the main component changes from the $\alpha + {}^{14}\mathrm{C}(2^+)$ channel to the $\alpha + {}^{14}\mathrm{C}_{\mathrm{g.s.}}$ channel (76%), and these channels have one higher nodal structure in their relative wave function ($N = 8$). Since the 0_2^+ state is not such a weakly bound state (binding energy of $\sim -2\,\mathrm{MeV}$), the tail of the $\alpha - {}^{14}\mathrm{C}$ relative wave function is not so extended in comparison to the usual cluster states, which appear at the energy close to the α-decay threshold [6]. According to the previous analysis in Ref. [29], the 0_2^+ state is identified as a four-particle–two-hole state, and this identification seems to be consistent with the cluster wave function with one higher nodal and shrunken tail structure.

Although the energy levels in the theory seem to agree with those in the experiments, the correspondence of the theory and the experiment is not perfect. This incompleteness is due

to the lack of the $\nu(1s0d)^2$ configuration in $^{18}\mathrm{O} = {}^{16}\mathrm{O} + N + N$. For example, the 0_3^+ state is missing in the present $\alpha + {}^{14}\mathrm{C}$ OCM calculation because the 0_3^+ state is considered to have the pure $^{16}\mathrm{O} \otimes \nu(1s_{1/2})^2$ configuration [12,29], which is completely out of the model space in the $\alpha + {}^{14}\mathrm{C}$ cluster configuration. In fact, the intrinsic configuration of 0_3^+ is identified as $(1s_{1/2})^2$ in Ref. [29], and it can be described by the $^{16}\mathrm{O} + N + N$ model [11,12]. These results mean that the energy positions of 0_2^+ and 0_4^+ are affected by the coupling with the $\nu(1s0d)^2$ configurations. Thus, the level assignment discussed in Fig. 1 may not be unique. Furthermore, the $\nu(1s0d)^2$ configuration generates the higher 0^+ resonance with $\nu(0d_{3/2})^2$, which will appear around the energy position of 0_5^+ as shown in the previous OCM calculation [14]. Thus, the inclusion of $\nu(1s0d)^2$ is significant in the complete level assignment of the theoretical calculation and the experimental observation.

Above the α threshold, two resonant states are realized as a result of the relative excitations from the bound two 0^+ states. The lower resonance 0_4^+ is generated by the relative excitation of $\alpha - {}^{14}\mathrm{C}_{\mathrm{g.s.}}$ from the 0_2^+ state, which keeps the dominance of the $\alpha + {}^{14}\mathrm{C}_{\mathrm{g.s.}}$ channel (94%), whereas the higher resonance 0_5^+, which has the dominance of $\alpha + {}^{14}\mathrm{C}(2^+)$ (57%), corresponds to the direct excitation from the ground 0_1^+ state. The relative wave functions of these resonant states have the one higher node in comparison to the respective bound states, and their tails are extended to the outer region because of the resonant feature embedded in the unbound continua. In other words, the resonant states have the dilute and extended α-cluster structures in comparison to the bound states. In this situation, the effect of the Coulomb interaction for the resonant states (0_4^+ and 0_5^+) is expected to be weaker than the effect for the bound states (0_1^+ and 0_2^+) in which the relative wave functions are confined in the region of the nuclear interaction.

Therefore, it is interesting to analyze the Coulomb shift in connection to the development of the α-cluster degrees of freedom. To investigate the Coulomb effect more clearly, we have extended the OCM calculation to the mirror system $^{18}\mathrm{Ne} = \alpha + {}^{14}\mathrm{O}$. In the calculation of ^{18}Ne, we have just replaced the charge in the Coulomb interaction, which is assumed to be the uniform sphere and slightly modified the nuclear interaction so as to reproduce the total binding energy with respect to the α threshold. The excitation energies and the decay widths in ^{18}O and ^{18}Ne are listed in Table I. On the proton-rich side (^{18}Ne), the decay width for the 0_4^+ and 0_5^+ states becomes broader due to the increase in the Coulomb repulsion. In addition, the excitation energy of the resonances in the proton-rich ^{18}Ne is more reduced than that in the neutron-rich ^{18}O.

TABLE I. Excitation energy (E_{ex}) and decay width (Γ_{R}) in ^{18}O and ^{18}Ne systems. The rightmost and middle columns show the results of ^{18}Ne and ^{18}O, respectively. B.S. and Res. are the abbreviations of bound state and resonant state, respectively.

	^{18}O		^{18}Ne	
	E_{ex}	Γ_{R}	E_{ex}	Γ_{R}
0_2^+ (B.S.)	4.3		4.3	
0_4^+ (Res.)	∼8.7	∼2.5	∼8.2	∼3.2
0_5^+ (Res.)	15.6	1.1	15.1	1.3

TABLE II. Energy shifts in the ^{18}O-^{18}Ne systems. The leftmost column shows the energy levels. In the middle and rightmost columns, the energy shift of ΔE_{Coul} with respect to the α threshold and the shift of excitation energy ΔE_{ex}, respectively, are shown. See the text for details.

	ΔE_{Coul}		ΔE_{ex}	
	Expt.	Th.	Expt.	Th.
0_1^+ (B.S.)	1.12	1.12	0	0
0_2^+ (B.S.)	1.06	1.14	0.06	0.03
0_4^+ (Res.)		0.53		0.58
0_5^+ (Res.)		0.65		0.46

The energy shifts of ^{18}O-^{18}Ne are summarized in Table II. In this table, ΔE_{Coul} represents the magnitude of the energy difference $\Delta E_{\mathrm{Coul}} = |E_{\mathrm{R}}({}^{18}\mathrm{O}) - E_{\mathrm{R}}({}^{18}\mathrm{Ne})|$ with respect to the α-decay threshold. As for the two bound states 0_1^+ and 0_2^+, the experimental (Expt.) energy shifts are reproduced by the theoretical (Th.) calculation, which amounts to about 1.1 MeV. The ΔE_{Coul} for the unbound resonances 0_4^+ and 0_5^+ are reduced to about half of the bound state, just about 0.6 MeV. This reduction is originated from the extended and dilute structure of the $\alpha - {}^{14}\mathrm{C}$ relative wave function. In the resonant states with the developed α-cluster structure, the relative wave functions have the main amplitude outside of the nuclear interaction region and can escape from the central part of the Coulomb interaction, whereas, in the bound state, the relative wave functions are confined inside of the nuclear interaction region and strongly feel the Coulomb interaction. Thus, the development of the α-cluster structures directly leads to the reduced Coulomb interaction.

This reduced energy shift with respect to the α threshold just corresponds to the reduction of the excitation energy, which is measured from the ground 0_1^+ state. In Table II, the shift of the excitation energies is shown by ΔE_{ex}, which is defined by $\Delta E_{\mathrm{ex}} = |E_{\mathrm{ex}}({}^{18}\mathrm{O}) - E_{\mathrm{ex}}({}^{18}\mathrm{Ne})|$ with the excitation energy of $E_{\mathrm{ex}} = E(0_{\mathrm{ex}}^+) - E(0_1^+)$. ΔE_{ex} is almost negligible for the bound 0_2^+ state, but it is enhanced to be about 0.5 MeV for the unbound resonant 0_4^+ and 0_5^+ states. The shift of the excitation energy corresponds to the so-called TES, which is originally discussed in the single-particle picture of $^{17}\mathrm{O} = {}^{16}\mathrm{O} + N$ and $^{17}\mathrm{F} = {}^{16}\mathrm{O} + P$ [2]. In the case of ^{17}O-^{17}F, the nucleon $1s_{1/2}$ state, existing just below the nucleon threshold, reveals the lower shift in the excitation energy because the extended $1s_{1/2}$ orbital state can avoid the Coulomb repulsion.

In the previous studies, the electric and isoscalar monopole transitions are discussed as the useful probes to identify the α-cluster formation [30]. In a naive mean-field picture, the monopole transition, such as $0_1^+ \to 0_{\mathrm{ex}}$, requires the $2\hbar\omega$ jump in the single-particle orbit. Since the $2\hbar\omega$ excitation is about 30–40 MeV in normal light nuclei, the single-particle strength must appear above the 30 MeV excitation energy.

TABLE III. Strength of electric monopole transitions in $^{18}\mathrm{O} = \alpha + {}^{14}\mathrm{C}$. All the strengths are shown in units of fm^2.

	Theory	Expt. [33]
0_2^+ (B.S.)	4.4	6.0
0_4^+ (Res.)	2.0	
0_5^+ (Res.)	6.3	

However, the strong monopole transition, which is comparable to the single-particle strength, appears below about 15 MeV, and this low-lying monopole strength can be naturally explained by the formation of the cluster structure [31]. In particular, the monopole transition is the most enhanced of all the excited states if the final state corresponds to the direct cluster excitation from the ground 0_1^+ state [32].

We check the strength of the electric monopole ($E0$) transition of $0_1^+ \to 0_f^+$ and compare the existing experimental data [33]. Here we calculate the contribution from the $\alpha - {}^{14}\mathrm{C}$ relative part to the $E0$ transition (without an elementary charge),

$$\hat{M}_{\mathrm{rel}}(E0) = \frac{4^2 \times 6 + 14^2 \times 2}{18^2} R^2, \tag{4}$$

where R denotes the $\alpha - {}^{14}\mathrm{C}$ radial coordinate [34]. Equation (4) is valid in the assumption of the common distribution of the proton and neutron densities. In Table III, the matrix elements of $\hat{M}_{\mathrm{rel}}(E0)$ are summarized.

The calculated $E0$ strength for $0_1^+ \to 0_2^+$ is 4.4 fm^2, and this value is almost the same as the experimental strength, such as 6.0 fm^2 measured from π decay [33]. The single-particle strength $[m_{\mathrm{s.p.}}(E0)]$ for the transition of $0p \to 1p$ is about 4.2 fm^2, which is evaluated by $m_{\mathrm{s.p.}}(E0) = \sqrt{5/8\nu^2}$ with $\nu = 0.187\,\mathrm{fm}^{-2}$ [30]. Therefore, all the excited states have the strength comparable to the single-particle strength. This is consistent with the previous studies about the monopole transition [30,31]. In particular, the $E0$ strength for $0_1^+ \to 0_5^+$ is the most enhanced, which reaches 1.5 times larger than the single-particle strength. This is because the 0_5^+ state corresponds to the direct cluster excitation from the ground 0_1^+ state as shown in Fig. 2, and the relative wave functions in the 0_1^+ state multiplied by R^2 have a good overlap with the wave function of the final 0_5^+ state.

IV. SUMMARY

To summarize, we have investigated the $J^\pi = 0^+$ energy spectra in $^{18}\mathrm{O} = \alpha + {}^{14}\mathrm{C}$ by applying the OCM under the ABC. The OCM + ABC calculation for ^{18}O nicely reproduces the observed $J^\pi = 0^+$ levels from the bound to the unbound region except for the 0_3^+ state, which is considered to be out of the α-cluster model space. The present result means that a large part of the $J^\pi = 0^+$ levels below $E_{\mathrm{ex}} = 15$ MeV can be described by the excitation of the α-cluster degrees of freedom; specifically, the 0_2^+ state is generated by the rearrangement of the cluster mixture from the ground 0_1^+ state, whereas two resonances are realized as the excitation of the cluster relative motion from the bound 0_1^+ and 0_2^+ states. Although the α-cluster degree of freedom plays an important role for the 0^+ level formation, it is still significant to include the two-neutron $\nu(1s0d)^2$ configuration around the ^{16}O core in the complete analysis of the 0^+ level scheme. The inclusion of the two-neutron configuration is now under progress.

The OCM + ABC calculation is also extended to $^{18}\mathrm{Ne} = \alpha + {}^{14}\mathrm{O}$, and the Coulomb shift for the mirror systems of ^{18}O-^{18}Ne is investigated. The Coulomb shift, which is measured from the α-decay threshold, is large for the bound 0_1^+ and 0_2^+ states, but it is reduced to be half for the 0_4^+ and 0_5^+ states. This reduction of the Coulomb shift is originated from the extended and dilute structure in the $\alpha - {}^{14}\mathrm{C}$ (^{14}O) relative wave function, which involves a large mixture of S-wave components. The reduced Coulomb shift in the cluster states corresponds to the compression of the excitation energy in the proton-rich ^{18}Ne. The origin of this compressed energy is just similar to the TES, which is discussed in $^{17}\mathrm{O} = {}^{16}\mathrm{O} + N$ and $^{17}\mathrm{F} = {}^{16}\mathrm{O} + P$ [2]. Thus, the energy compression predicted in the cluster system should be called the "cluster TES." We propose that the cluster TES is a new probe to identify the extended and dilute structure of the cluster configuration.

Furthermore, the strength of the electric monopole ($E0$) transition, which is another probe to identify the cluster excitation, is calculated. In accordance with the previous studies [30,31], all the energy levels have the $E0$ strength comparable to the single-particle excitation, which requires much higher excitation energy than the energy of the cluster excitation. In particular, the strength going to the 0_5^+ state is the most enhanced of all the excited states because this state corresponds to the direct cluster excitation from the ground state [32]. Therefore, we can clearly identify evidence of the cluster excitation from the ground state by combining the cluster TES and the monopole strength: the lower shift of the excitation energy and the enhanced monopole strength.

We have focused on the 0^+ states to pin down the suppressed Coulomb shift induced by the α clustering. However, there are other states with finite spins in ^{18}O, which are considered to have the α-cluster structure. The Coulomb shift should be analyzed in such a finite spin state. In particular, the analysis of the 1^- states is interesting because the recent works have predicted that the isoscalar dipole (IS1) transition of $0_1^+ \to 1^-$ is enhanced by the development of the α-cluster structure [35,36]. The combined analysis of the Coulomb shift and the IS1 transition is an interesting subject.

The present calculation strongly suggests that not only the analysis of the neutron-rich systems, but also the analysis of the proton-rich ones is quite useful in the experimental probe for the cluster degrees of freedom. Unfortunately, the experimental information relevant to the unbound region is insufficient in the proton-rich system of ^{18}Ne, although the candidates of 0^+ resonances are suggested around $E_{\mathrm{ex}} \sim 8$ MeV in $^{14}\mathrm{O}(\alpha, p)\,^{17}\mathrm{F}$ [37], which seems to be consistent with the present calculation. Thus, the experimental investigation of the unbound resonance in ^{18}Ne is an important subject in future experiments.

Furthermore, the present result about the cluster TES is also possible to occur in more general $N \neq Z$ systems. For example, it is interesting to consider the $4N$ nuclear system with two extra nucleons, such as ^{10}Be-^{10}C, ^{14}C-^{14}O,

and ^{22}Ne-^{22}Mg. In particular, the reduction of the Coulomb shift will be prominent in the exotic cluster states, which have dilute gaslike structures [38] or linear chain structures [39] because these exotic structures involve the large spatial extension. In advancing the study of the cluster TES, it is essential to investigate the level structure, especially the unbound resonances, experimentally. The experimental analysis of the resonant structures on the proton-rich side is strongly desired.

ACKNOWLEDGMENTS

We would like to thank S. Sonoda and all the members of the Quantum Many-body Physics Laboratory at Kansai University for their useful discussions and kind support. One of the authors (M.I.) thanks Prof. K. Kato and Prof. M. Kimura at Hokkaido University, H. G. Masui at the Kitami Institute of Technology, N. Itagaki at YITP, and P. Descouvemont at ULB for their valuable discussions, useful comments, and encouragement.

[1] I. Tanihata, H. Savajolo, and R. Kanungo, Prog. Part. Nucl. Phys. **68**, 215 (2013).
[2] A. Bohr and B. R. Mottelson, *Nuclear Structure* (Benjamin, New York, 1969), Vol. I, p. 320.
[3] K. Ikeda *et al.*, Prog. Theor. Phys. Suppl. **68**, 1 (1986).
[4] H. Horiuchi *et al.*, Suppl. Prog. Theor. Phys. **192**, 1 (2012) and references therein.
[5] M. Freer, Rep. Prog. Phys. **70**, 2149 (2007).
[6] K. Ikeda *et al.*, Prog. Theor. Phys. Suppl. **E68**, 464 (1968).
[7] M. Ito, EPJ Web Conf. **122**, 09002 (2016).
[8] P. Descouvemont and D. Baye, Phys. Rev. C **31**, 2274 (1985).
[9] N. Furutachi *et al.*, Prog. Theor. Phys. **119**, 403 (2008).
[10] M. Ito, JPS Conf. Proc. **6**, 030033 (2015).
[11] N. Michel, W. Nazarewicz, M. Ploszajczak, and J. Okolowicz, Phys. Rev. C **67**, 054311 (2003).
[12] H. Masui, K. Kato, and K. Ikeda, Phys. Rev. C **75**, 034316 (2007).
[13] A. Saito, Suppl. Prog. Theor. Phys. **62**, 11 (1977).
[14] H. Furutani, H. Kanada, T. Kaneko, S. Nagata, H. Nishioka, S. Okabe, S. Saito, T. Sakuda, and M. Seya, Suppl. Prog. Theor. Phys. **68**, 279 (1980).
[15] M. Nakao, H. Umehara, S. Sonoda, S. Ebata, and M. Ito, EPJ Web Conf. **163**, 00040 (2017).
[16] J. P. Elliott, Proc. R. Soc. London, Ser. A **245**, 128 (1958); **245**, 562 (1958); M. Harvey, *Advances in Nuclear Physics*, edited by M. Baranger and E. W. Vogt (Plenum, New York, 1968), Vol. 1, p. 67.
[17] M. Ito, Y. Hirabayashi, and Y. Sakuragi, Phys. Rev. C **66**, 034307 (2002) and references therein.
[18] A. Ozawa, T. Suzuki, and I. Tanihata, Nucl. Phys. A **693**, 32 (2001).
[19] A. M. Kobos, B. A. Brown, P. E. Hodgson, G. R. Satchler, and A. Budzanowski, Nucl. Phys. A **384**, 65 (1982); A. M. Kobos, B. A. Brown, R. Lindsay, and G. R. Satchler, *ibid.* **425**, 205 (1984).
[20] M. El-Azab Farid and G. R. Satchler, Nucl. Phys. A **438**, 525 (1985).
[21] M. E. Brandan and G. R. Satchler, Nucl. Phys. A **487**, 477 (1988).
[22] K. Egashira, K. Minomo, M. Toyokawa, T. Matsumoto, and M. Yahiro, Phys. Rev. C **89**, 064611 (2014).
[23] M. Ito and K. Yabana, Prog. Theor. Phys. **113**, 1047 (2005).
[24] Y. Takenaka, R. Otani, M. Iwasaki, K. Mimura, and M. Ito, Prog. Theor. Exp. Phys. **2014**, 113D04 (2014).
[25] M. Iwasaki, R. Otani, Y. Takenaka, and M. Ito, Prog. Theor. Exp. Phys. **2015**, 023D01 (2015).
[26] J. Vernotte, G. Berrier-Ronsin, J. Kalifa, and R. Tamisier, Nucl. Phys. A **390**, 285 (1982).
[27] M. L. Avila, G. V. Rogachev, V. Z. Goldberg, E. D. Johnson, K. W. Kemper, Y. M. Tchuvil'sky, and A. S. Volya, Phys. Rev. C **90**, 024327 (2014).
[28] W. von Oertzen *et al.*, Eur. Phys. J. A **43**, 17 (2010).
[29] R. L. Lowson, F. J. D. Serduke, and H. T. Fortune, Phys. Rev. C **14**, 1245 (1976).
[30] T. Yamada, Y. Funaki, H. Horiuchi, K. Ikeda, and A. Tohsaki, Prog. Theor. Phys. **120**, 1139 (2008).
[31] T. Yamada, Y. Funaki, T. Myo, H. Horiuchi, K. Ikeda, G. Röpke, P. Schuck, and A. Thosaki, Phys. Rev. C **85**, 034315 (2012).
[32] M. Ito, Phys. Rev. C **83**, 044319 (2011); M. Ito and K. Ikeda, Rep. Prog. Phys. **77**, 096301 (2014).
[33] K. H. Souw *et al.*, Phys. Rev. C **11**, 1899 (1975).
[34] H. Sagawa, N. Takigawa, and N. van Giai, Nucl. Phys. A **543**, 575 (1992).
[35] Y. Chiba, M. Kimura, and Y. Taniguchi, Phys. Rev. C **93**, 034319 (2016).
[36] Y. Chiba, Y. Taniguchi, and M. Kimura, Phys. Rev. C **95**, 044328 (2017).
[37] A. Kim, N. H. Lee, M. H. Han, J. S. Yoo, K. I. Hahn, H. Yamaguchi, D. N. Binh, T. Hashimoto, S. Hayakawa, D. Kahl, T. Kawabata, Y. Kurihara, Y. Wakabayashi, S. Kubono, S. Choi, Y. K. Kwon, J. Y. Moon, H. S. Jung, C. S. Lee, T. Teranishi, S. Kato, T. Komatsubara, B. Guo, W. P. Liu, B. Wang, and Y. Wang, Phys. Rev. C **92**, 035801 (2015).
[38] T. Yamada and Y. Funaki, Phys. Rev. C **82**, 064315 (2010).
[39] T. Baba and M. Kimura, Phys. Rev. C **94**, 044303 (2016).